Azerbaijan University of Architecture and Construction
ISSN 2706-7726
Engineering Mechanics
Scientific and Technical Journal
E-mail: engineeringmechanics@azmiu.edu.az

September 2025 Issue 21 Volume 13 Number 3 Pages 37-45

Evaluation of the accuracy of material deformation diagrams for compressed circular reinforced concrete elements based on a nonlinear deformation model

Hajiyeva U.M.
«OilGasScientificResearchProject» Institute, SOCAR, Baku, Azerbaijan
hajiyevmukhlis60@gmail.com

Abstract: In the application of the nonlinear deformation model, which is considered the modern calculation methodology of reinforced concrete structures, design codes propose the use of material diagrams described by various analytical expressions. The main purpose of the article is to evaluate the results obtained based on these simplified bilinear and trilinear diagrams. The author has developed methodologies for investigating the stress–strain state and load-bearing capacity of concrete under compression using both simplified and full diagrams proposed by Eurocode (EC). In all variants, it is assumed that reinforcement bars deform according to a bilinear diagram. By applying this methodology, numerical examples are presented where results obtained from different diagrams are compared, showing that although similar results are achieved in determining load-bearing capacity across all variants, other parameters characterizing the stress–strain state are determined more accurately with the trilinear diagram.
Keywords: nonlinear deformation model, concrete, reinforcement, load-bearing capacity, eccentricity.

Introduction

In recent years, the modern theory of reinforced concrete structures has been intensively developed through the application of the nonlinear deformation model [1,2,3]. In accordance with the principles of this model, when calculation methodologies are established, the nonlinear deformation diagrams of materials and the validity of the plane section hypothesis up to the moment of failure for complex reinforced concrete structures are accepted. Unlike the limit state method, the application of this model allows the investigation of the stress–strain state for any arbitrary level of loading [2,3,4,5,6,7]. One of the compressed reinforced concrete structural elements is the column with a circular cross-section, uniformly reinforced along the section. It is known that parameters such as the eccentricity of the compressive force and the slenderness of the compressed element must be considered as factors influencing the stress–strain state and load-bearing capacity of such elements. Depending on these quantities, the load-bearing capacity of the compressed element is determined by either the strength or stability condition. To clarify which condition defines the load-bearing capacity, the “load–displacement” diagram of the compressed element must be known. Modern calculation methodologies allow the investigation of both the stress–strain state and the load-bearing capacity based on a unified methodology depending on the level of loading [2,3,4,5,6,7]. In this article, based on the calculation

methodology proposed by the author, the accuracy of various simplified diagrams suggested by standards is evaluated through numerical experiments.

Problem Statement

For a reinforced concrete element with a circular cross-section, compressed with arbitrary eccentricity and arbitrarily reinforced, a system of governing equations is established to investigate the stress–strain state by applying a bilinear diagram for reinforcement bars, a bilinear and trilinear simplified diagram for concrete as proposed in construction codes, and the full diagram suggested in Eurocode. When forming the system of equations, it is assumed that the plane section hypothesis remains valid for the composite section up to the moment of loss of load-bearing capacity. The tensile behavior of concrete is neglected in comparison with its compressive behavior, and it is assumed that the tensile stresses in the section are carried by the reinforcement bars distributed across the section [2-9]. Finally, the solution of the problem reduces to solving a system of nonlinear algebraic equations with respect to the deformation of concrete at the compressed face of the most stressed section and the parameters determining the position of the neutral axis.

Solution of the Problem

In Figure 1 below, the possible stress–strain states that may form in the section when applying the full diagram are illustrated. For concrete in compression, the bilinear, trilinear, and full diagrams, and for reinforcement bars in tension–compression, the bilinear diagrams are presented in Table 1. Furthermore, in Table 2, the analytical expressions of these deformation diagrams of the materials are given. The parameters included in these analytical expressions are determined by construction codes. Their characteristic values are provided at the same table.

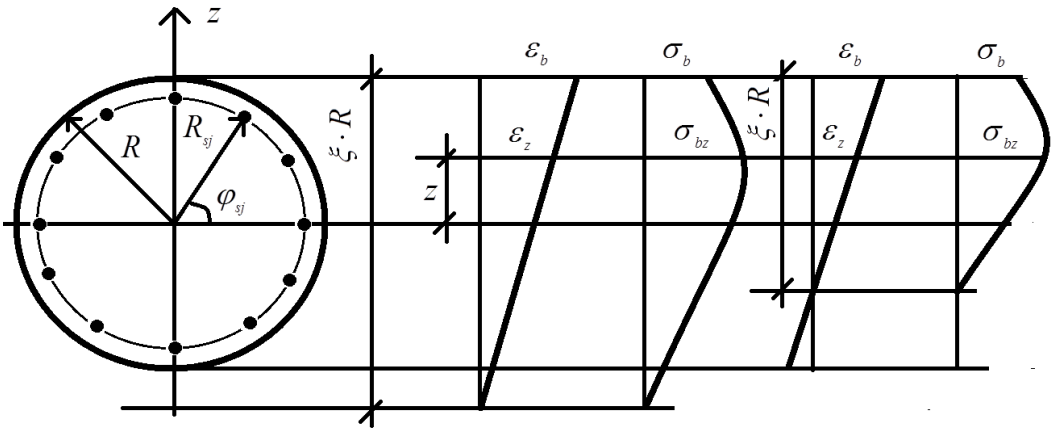

Figure 1. Calculation scheme of the cross-section of a reinforced concrete element with circular cross-section.

Table 1. Deformation diagrams of materials.

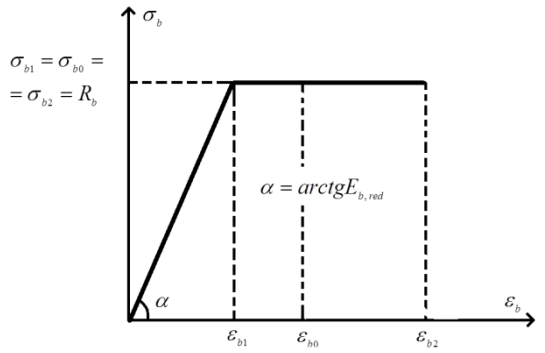	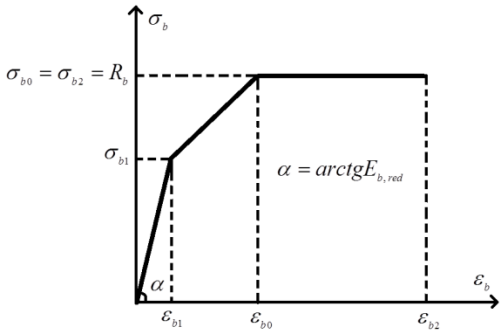
Bilinear diagram of concrete in compression	Trilinear diagram of concrete in compression
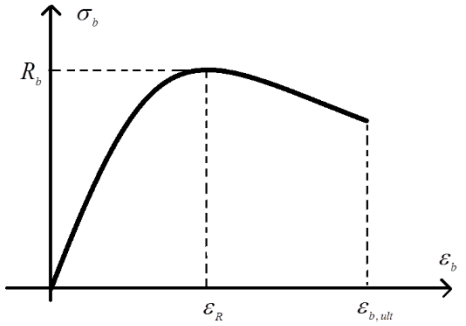	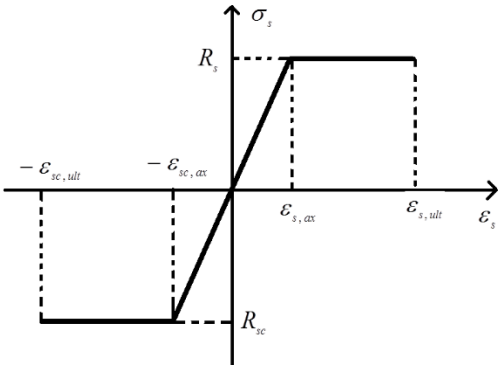
Full diagram of concrete in compression	Bilinear diagram of reinforcement bars in tension–compression
$\varepsilon_{b1} = 0{,}0015$; $\varepsilon_{b0} = 0{,}002$; $\varepsilon_{b2} = 0{,}0035$; $\sigma_{b1} = 0{,}6 \cdot R_b$	

Table 2. Analytical expressions of material deformation diagrams.

Diagram for material	Analytical expression of the "stress–strain" diagram
Bilinear diagram of concrete in compression	$\sigma_b(z) = \begin{cases} E_{b,red} \cdot \varepsilon_{bz} ; & if \quad 0 \le \varepsilon_{bz} \le \varepsilon_{b1} \\ R_b ; & if \quad \varepsilon_{b1} < \varepsilon_{bz} \le \varepsilon_{b2} \end{cases}$ (1)
Trilinear diagram of concrete in compression	$\sigma_{bz}(\varepsilon_b, x) = \begin{cases} \frac{\sigma_{b1}}{\varepsilon_{b1}} \cdot \varepsilon_{bz} ; & if \quad 0 \le \varepsilon_b \le \varepsilon_{b1} \\ \sigma_{b1} + \frac{R_b - \sigma_{b1}}{\varepsilon_{b0} - \varepsilon_{b1}} \cdot (\varepsilon_{bz} - \varepsilon_{b1}); & if \quad \varepsilon_{b1} < \varepsilon_b \le \varepsilon_{b0} \\ R_b ; & if \quad \varepsilon_{b0} < \varepsilon_{bz} \le \varepsilon_{b2} \end{cases}$ (2)
Full diagram of concrete in compression	$\sigma_{bz}(\varepsilon_b, x) = R_b \cdot \frac{k \cdot \varepsilon_{bz} - \varepsilon_{bz}^2}{1 + (k-2) \cdot \varepsilon_{bz}}$ (3)
Bilinear diagram of reinforcement in tension–compression	$\sigma_{sj}(\varepsilon_b, x) = \begin{cases} E_{sj} \cdot \varepsilon_{sj}(\varepsilon_b, x); & if \quad \lvert \varepsilon_{sj} \rvert \le \varepsilon_{sj,ax} \\ R_{sj} \cdot sign(\varepsilon_{sj}); & if \quad \lvert \varepsilon_{sj} \rvert > \varepsilon_{sj,ax} \end{cases}$ (4)

Since, in accordance with the requirements of the nonlinear deformation model, it is accepted that the plane section hypothesis remains valid for the composite reinforced concrete section up to the moment of failure, based on this hypothesis the distribution of deformation across the section is expressed in terms of the deformation at the compressed face of the section and the parameters determining the position of the neutral axis, see Figure 1.

$$\varepsilon_{bz} = \frac{\varepsilon_b}{x} \cdot (x - R + z). \tag{5}$$

Based on this equality, and using the dependencies given above in Table 2, the value of the compressive stresses arising in the concrete within the cross-section of the reinforced concrete element can be uniquely determined by the parameters ε_b and x. Moreover, according to the fourth equality, the stresses in the reinforcement bars also become functions of these two parameters. Considering the compressive stresses arising in the concrete, the internal normal force and bending moment formed in the section can be expressed through the corresponding formulas of material resistance as follows:

$$N_b(\varepsilon_b, x) = 2 \cdot \int_q^R \sigma_{bz}(\varepsilon_b, x) \cdot \sqrt{R^2 - z^2}\, dz\ ; \tag{6}$$

$$M_b(\varepsilon_b, x) = 2 \cdot \int_q^R \sigma_{bz}(\varepsilon_b, x) \cdot z \cdot \sqrt{R^2 - z^2}\, dz \tag{7}$$

Depending on the position of the neutral axis, the lower limit of these integrals is defined as in $q = \begin{cases} -R\ ; & if \quad x \geq 2R \\ R - x\ ; & if \quad x < 2R \end{cases}$ (8). In the same way, based on the stresses in the reinforcement bars, the following analogous equalities can be written for the internal normal force and bending moment formed in the section:

$$N_s(\varepsilon_b, x) = \sum_{j=1}^{k_s} \sigma_{sj}(\varepsilon_b, x) \cdot A_{sj}\ ; \tag{9}$$

$$M_s(\varepsilon_b, x) = \sum_{j=1}^{k_s} \sigma_{sj}(\varepsilon_b, x) \cdot A_{sj} \cdot r_{sj} \cdot \sin\varphi_{sj} \tag{10}$$

In these equalities, A_{sj} - is the cross-sectional area of the corresponding reinforcement bar. In the case of eccentric compression, by approximating the bent axis of the compressed element with a half-wave of the sine function $w(y) = f \cdot \sin\frac{\pi \cdot y}{l_0}$, it becomes possible to relate the maximum displacement of the compressed element to the parameters ε_b and x as follows:

$$f = \rho_* \cdot \frac{\varepsilon_b}{x}, \quad \rho_* = \frac{l_0^2}{\pi^2} \tag{11}$$

In these equalities, l_0 - is the calculated length of the compressed element. Based on the obtained expressions, for the most stressed middle section of the compressed element, the following equilibrium equations can be written:

$$N_b(\varepsilon_b, x) + N_s(\varepsilon_b, x) = P \tag{12}$$

$$M_b(\varepsilon_b, x) + M_s(\varepsilon_b, x) = P \cdot \left(e + \rho_* \cdot \frac{\varepsilon_b}{x}\right) \tag{13}$$

The obtained equations (12) and (13) form the main decisive nonlinear system of equations for the problem under consideration. In these equalities, e - is the eccentricity of the compressive force, and P - is the force compressing the element. Since it is not possible to construct an analytical solution for this system, the numerical solution algorithm proposed by Prof. M.A.Hajiyev is applied. Based on this algorithm, it is possible to determine with any desired accuracy the parameters characterizing the stress–strain state at an arbitrary level of loading. By eliminating the force parameter from the obtained system of equations, the following equality can be written, which establishes a relationship between the parameters ε_b and x:

$$\Phi(\varepsilon_b, x) = M_b(\varepsilon_b, x) + M_s(\varepsilon_b, x) - (M_b(\varepsilon_b, x) + M_s(\varepsilon_b, x)) \cdot \left(e + \rho_* \cdot \frac{\varepsilon_b}{x} \right) = 0 \qquad (14)$$

Since the variation interval of the parameter ε_b is known in advance, we accept the value ($0 \le \varepsilon_b \le \varepsilon_{b2} = 0{,}0035$) and from equation (14) the parameter x, which determines the position of the neutral axis, can be found with any desired accuracy as the root of a single-variable nonlinear equation. Based on the known values of these two parameters, all the parameters characterizing the stress–strain state, including the maximum displacement f of the element and the compressive force P corresponding to the accepted deformation value, can be determined. This makes it possible to construct the "load–displacement" graphs, which play an important role in determining the load-bearing capacity of compressed elements. The described solution algorithm can be easily programmed, and a corresponding program module has been developed in the Turbo Pascal ABC algorithmic language to implement the solution algorithm. Using this module, various parametric analyses have been carried out.

Parametric analyses

Initial data – radius $R = 0{,}2\ m$ of the cross-section, calculated length $l_0 = 6\ m$ of the element, the section reinforced with $A400$ class $12 \varnothing 22$ reinforcement, radius $R_{sj} = 0{,}169\ m$ of the circle on which the centroids of the reinforcement bars are located, design resistance $R_s = R_{sc} = 360\ MPa$ of the reinforcement bars in tension–compression, concrete class $B\,20$, design compressive resistance $R_b = 11{,}5\ MPa$ of the concrete. In the case of conditional central compression, that is, when the eccentricity of the compressive force is $e = 0{,}01\ m$, the corresponding calculations have been carried out. As a result of these calculations, in Figure 2 the "load–displacement" diagrams have been constructed.

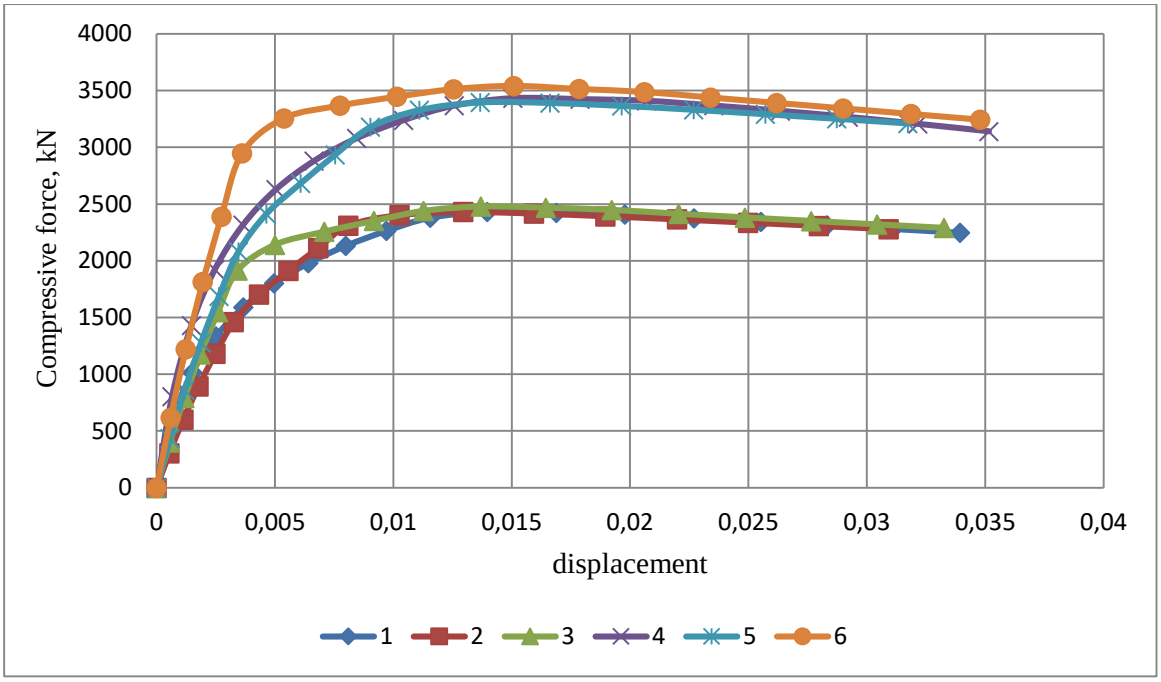

Figure 2. "Load–displacement" diagrams of the compressed element with the calculated length $l_0 = 6\ m$.

1 – Complete compressive diagram for concrete $B\ 20$; 2 – Tri-linear compressive diagram for concrete $B\ 20$; 3 – Bi-linear compressive diagram for concrete $B\ 20$; 4 – Complete compressive diagram for concrete $B\ 40$; 5 – Tri-linear compressive diagram for concrete $B\ 40$; 6 – Bi-linear compressive diagram for concrete $B\ 40$;

As a result of the calculations carried out, it was determined that when applying the complete, three-line, and two-line diagrams of concrete in compression, the corresponding values $P_{cr}^{(1)} = 2431,948\ kN$, $P_{cr}^{(2)} = 2430,317\ kN$, $P_{cr}^{(3)} = 2477,955\ kN$ and were obtained for the critical forces. This shows that, compared with the complete diagrams, the tri-linear and bi-linear diagrams give errors of $-0,0067\ \%$ and $0,0019\ \%$, respectively, in determining the load-bearing capacity. In addition, for other parameters characterizing the stress–strain state at the moment of loss of load-bearing capacity, the value $\varepsilon_b^{(1)} = 0,002$, $f_{cr}^{(1)} = 0,013967\ m$, $x_{cr}^{(1)} = 0,5223\ m$, $\varepsilon_b^{(2)} = 0,0022$, $f_{cr}^{(\ )} = 0,012951\ m$, $x_{cr}^{(2)} = 0,6196\ m$, $\varepsilon_b^{(3)} = 0,002$, $f_{cr}^{(3)} = 0,013695\ m$, $x_{cr}^{(3)} = 0,5327\ m$ were obtained. From this, when the complete diagram and the two-line diagram are applied, the increasing branch of the complete diagram is fully realized, while when the three-line diagram is applied, the descending branch is also realized.

In order to study the effect of the concrete grade, the same element of calculated length was analyzed for concrete grades $B\ 40$ and $R_b = 22\ MPa$, and the results are presented in Graph 1. As can be seen from the graphs, although the load-bearing capacities according to all three diagrams are close to each other, other parameters characterizing the stress–strain state may differ. Results obtained with the application of the three-line diagram are observed to be closer to those obtained with the complete diagram. In Figure 3, the variation of the parameter determining the position of the neutral axis according to the level of loading is presented for all three diagrams. From the constructed graphs the analytical expression of the concrete's compression deformation diagram has a more significant influence on the variation of this parameter. It was also determined that, when the complete diagram and the two-line diagram are applied, now of loss of load-bearing capacity the third and fourth reinforcement bars reach

the yield limit, while the remaining reinforcement bars work within the elasticity limit. However, when the three-line diagram is applied, in addition the second reinforcement bar also reaches the yield limit.

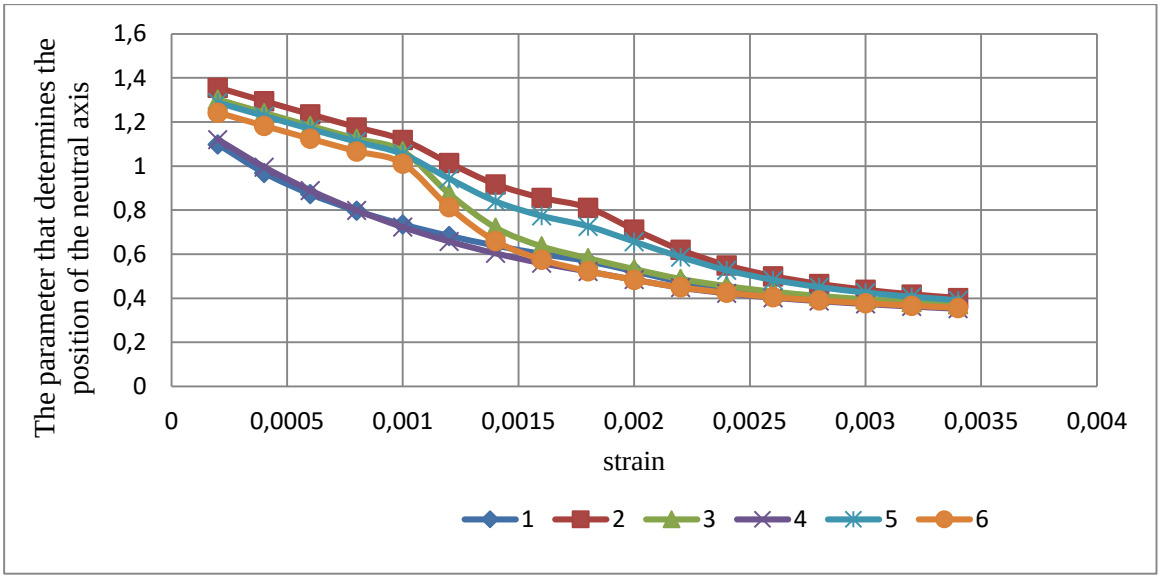

Figure 3. The dependence graph of the parameter $l_0 = 6\ m$ which determines the position of the neutral axis in the most stressed cross-section of the compressed element of length x, on the deformation E of the compressed face of that section.

1 – Complete compressive diagram for concrete $B\ 20$;

2 – Tri-linear compressive diagram for concrete $B\ 20$;

3 – Bi-linear compressive diagram for concrete $B\ 20$;

4 – Complete compressive diagram for concrete $B\ 40$;

5 – Tri-linear compressive diagram for concrete $B\ 40$;

6 – Bi-linear compressive diagram for concrete $B\ 40$;

From the graphs it is clearly seen that, although the change of the parameter x, which determines the position of the neutral axis, is small when the concrete grade increases from $B\ 20$ to $B\ 40$, the load-bearing capacity of the element increases by approximately 41.1%. This once again shows that one of the main factors affecting the load-bearing capacity of compressed reinforced concrete elements is the grade of the concrete.

To study the effect of the slenderness of the compressed element, the above-considered element was also analyzed for an element with the calculated length $l_0 = 3\ m$, while keeping all other parameters the same. The results of the calculations are reflected in figure 4 and figure 5 below. From these graphs it is also clearly seen that, when applying all three diagrams, almost the same results are obtained for the load-bearing capacity. Here too, although the increase of the concrete grade has little effect on the change of the parameter that determines the position of the neutral axis, it has a significant effect on the load-bearing capacity. For the short element considered, the increase in load-bearing capacity amounted to approximately 42.4%. It should be noted that, because of the calculations carried out, it was determined that the reinforcement ratio, the eccentricity of the compressive force, and the method of fixing the ends of the compressed element also have a significant effect on the load-bearing capacity. It was also determined that, under the influence of service loads, the application of the complete diagram is recommended to obtain more reliable results.

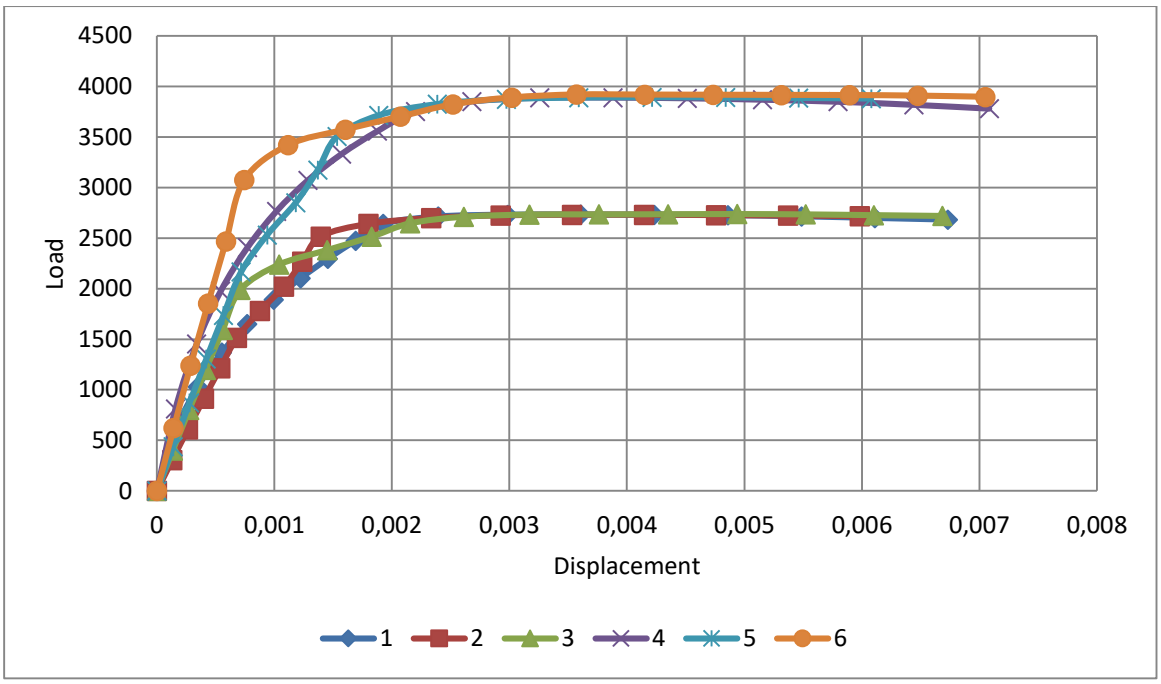

Figure 4. ‘Load–displacement’ graphs of the compressed element with the calculated length $l_0 = 3\ m$.

1 – Complete compressive diagram for concrete $B\ 20$;

2 – Tri-linear compressive diagram for concrete $B\ 20$;

3 – Bi-linear compressive diagram for concrete $B\ 20$;

4 – Complete compressive diagram for concrete $B\ 40$;

5 – Tri-linear compressive diagram for concrete $B\ 40$;

6 – Bi-linear compressive diagram for concrete $B\ 40$;

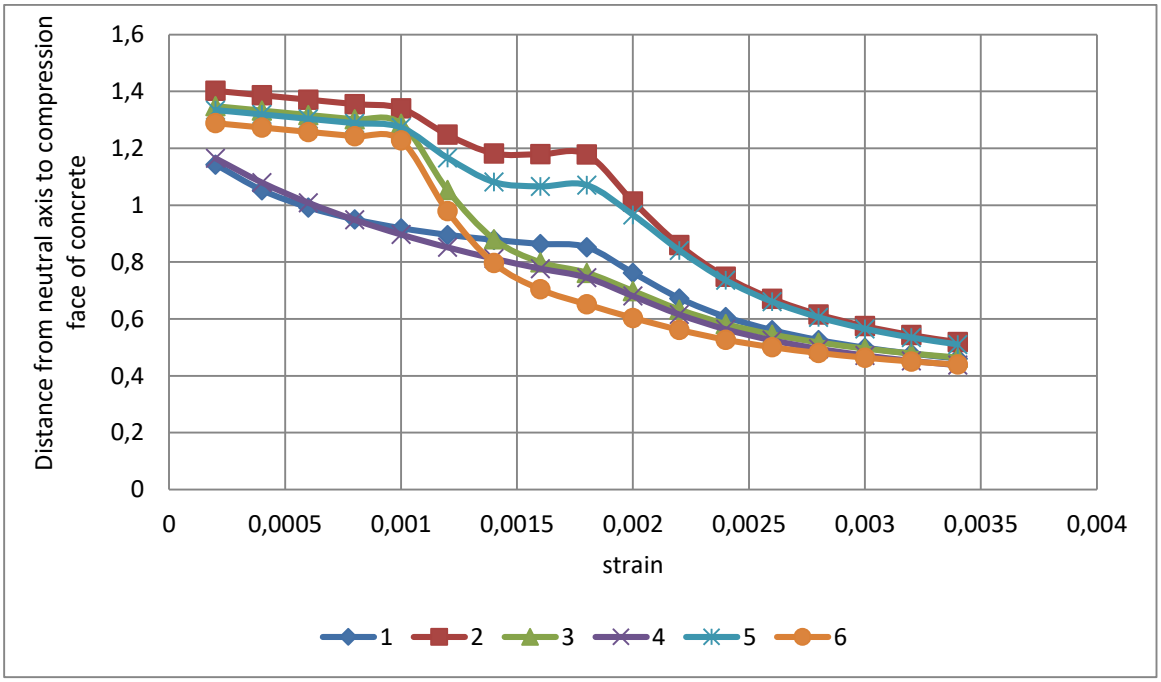

Figure 5. The dependence graph of the parameter $l_0 = 3\ m$, which determines the position of the neutral axis in the most stressed cross-section of the compressed element of length x, on the deformation ε_b of the compressed face of that section.

1 – Complete compressive diagram for concrete B 20 ;

2 – Tri-linear compressive diagram for concrete B 20 ;

3 – Bi-linear compressive diagram for concrete B 20 ;

4 – Complete compressive diagram for concrete B 40 ;

5 – Tri-linear compressive diagram for concrete B 40 ;

6 – Bi-linear compressive diagram for concrete B 40 ;

Main results.

1. In determining the load-bearing capacity of compressed reinforced concrete elements, when using the simplified bilinear and trilinear diagrams proposed by the standards, results consistent with those obtained by applying the complete diagram are achieved.
2. For the reliable determination of the parameter characterizing the stress–strain state of compressed elements, the application of more precise deformation diagrams is recommended.

Reference

1.Колмогоров А.Г., Плевков В.С. Расчет железобетонных конструкций по российским и зарубежным нормам. Москва, АСВ, 2015 – 512 с.

2. Hajiyev, M. A., Huseynov, I. G., Hajiyeva, U. M., & Bashirzade, S. R. (2026). A Novel Approach to Long-Term Load-Carrying Capacity Assessment of Circular Reinforced Concrete Support Structures Considering Hereditary Creep. SOCAR Proceedings No.1 (2026) 116-124. http://dx.doi.org/10.5510/OGP20260101159

3. Hajiyev, M. A., Huseynov, I. G., Hajiyeva, U. M., & Bashirzade, S. R. (2025). Structural Performance of Marine Circular Reinforced Concrete Piers Under Axial Loading. SOCAR Proceedings No.2. 124-134. http://dx.doi.org/10.5510/OGP20250201073

4. Hajiyev, M. A., Huseynov, I. G., Hajiyeva, U. M., & Alaeva, S. M. (2024). Calculation of metal elements deflection using a three-line strain diagram. SOCAR Proceedings, 2, 109-114. http://dx.doi.org/10.5510/OGP20240200975

5.Гаджиев, М. А., Гусейнов, И. Г., & Гаджиева, У. М. (2023). Напряженно-Деформированное Состояние И Несущая Способность Сжатых Трубобетонных Элементов. SOCAR Proceedings Special Issue No. 1 (2023) 021-026. http://dx.doi.org/10.5510/OGP2023SI100836

6. Hajiyeva, U. M. (2021). Nonlinear Deformation Analysis of Compressed Reinforced Concrete Elements of Circular Cross-section. Herald of Azerbaijan Engineering Academy, 13(4), 47-57.

7. Гаджиева, У. М. (2021). Расчет железобетонных элементов круглого поперечного сечения по нелинейной деформационной модели. Эксперт: теория и практика, (5), https://cyberleninka.ru/article/n/raschet-szhatyh-zhelezobetonnyh-elementov-kruglogo-poperechnogo-secheniya-po-nelineynoy-deformatsionnoy-modeli

8. Hajiyev, M. A., Aeinehchi, S., Bashirzade, S. R., Asadov, E. Z., & Khalilov, H. A. (2024). Study on the flexural performance of reinforced concrete structures strengthened with composites. Scientific and Technical Journal on Engineering Mechanics, 8(2), 16.

9. Гарибов, Р. Б., Гаджиева, У. М., & Баширзаде, С. Р. (2018). К вопросу об оценке безопасности и долговечности проектируемых железобетонных конструкций. Вестник Волжского регионального отделения Российской академии архитектуры и строительных наук, (21), 160-164.